2022 17th International Conference on
Control, Automation, Robotics and Vision (ICARCV)
December 11-13, 2022. Singapore

Optimal RTGC Controller using Robust PID H_∞ Integral-Backstepping under Payload Mass and Rope Length Uncertainties*

Steven Bandong, Yul Yunazwin Nazaruddin and Endra Joelianto

2022 17th International Conference on Control, Automation, Robotics and Vision (ICARCV) | 978-1-6654-7687-4/22/$31.00 ©2022 IEEE | DOI: 10.1109/ICARCV57592.2022.10004328

Abstract— **The increase in goods traffic between countries and islands requires the availability of port automation so that the distribution of goods is faster and the quality is guaranteed. One of the control problems for automating the port is controlling the position and sway angle of the container on the Rubber Tyred Gantry Crane (RTGC). However, the RTGC system's model is often uncertain because of the uncertainty in the mass of the payload and the length of the hauling rope when operating. This paper proposes a robust PID controller based on H_∞ integral backstepping to overcome this problem. Particle Swarm Optimization (PSO), Simulated Annealing (SA) and Genetic Algorithms (GA) are used to optimize the parameter of H_∞ integral backstepping so that the system response follows the desired trajectory. The results show that the control system designed can provide a satisfactory solution to variations in the mass and length of the rope. PSO and SA give better optimal and robust performance than GA.**

Keywords: H_∞ integral backstepping, Robust PID, RTGC control system, Simulated Annealing, Particle Swarm Optimization, Genetic Algorithm

I. INTRODUCTION

Trade traffic between islands and continents is still very dependent on sea transportation even though air transportation routes have been available in this century. This statement was stated by [1] when researching trade traffic in Latin America, where 72-96% still use sea routes. Even from 2000 to 2019, there was an almost 4-fold increase in trade volume [2]. This data, of course, will directly impact the port's bustle, especially in the loading and unloading process of containers at the container yard. For example, at the port of Tanjung Priok, the loading and unloading process takes place every day for 24 hours [3]. However, this causes an increase in the potential for accidents due to fatigue, illness, or lack of experience of the rubber-tyred gantry crane (RTGC) operator, which is a container loading and unloading tool at the container yard. These problems lead to the need for RTGC control and automation.

The problem of RTGC control has two prominent cases that are often discussed by researchers: controlling the position and the sway angle of the container when it is moved. Several control methods have been applied to find a solution to this problem. Fuzzy has been used to control the position and sway angle by [4] while [5] combined fuzzy with PID controller to get better performance. [6] used LQR to make optimal control to minimize swing angle and position error. Several other studies have applied optimization techniques such as PSO, PFA, GA, etc., to find the optimal controller [7][8]. Although there are various control methods, in general, PID is the most frequently used controller due to its ease of application [9], and PID had also been used in various applications such as quadrotors [10], boilers [11], wind turbine [12] and others.

However, modelling errors or disturbances, uncertainty or parameter changes can result in the control system that has been designed not operating as intended. Therefore, apart from the need for an optimal control system, it is also necessary to develop a robust controller against various possible disturbances. H_∞ is a robust control method that has been used in various cases such as controlling trains [13], ships [14], and hydropower systems [15]. The H_∞ representation into a robust PID form by applying the backstepping method has been developed in [16]. This method has been used in various applications [13][15][16] and gave satisfactory results. In addition, this method has advantages from the application side because, generally, control tools support PID implementation.

In the RTGC system, uncertainty often occurs, namely the variation in the mass of the container and the length of the transport rope during the container transfer process. This paper proposes robust controller w.r.t variations of load mass and rope length using PID-H_∞ backstepping. Optimization of the H_∞ parameter will be carried out using the PSO, SA and GA methods so that the system can follow the desired position trajectory.

II. RTGC CONTROL MODEL

The 2D Gantry Crane system can be depicted in Fig.1. m_2 is the mass of the trolley. F is the driving force of the trolley by the DC motor. g is the force of gravity, l the length of the rope, x the position of the trolley, θ is the angle of swing and m_1 is the mass of the load in this case is a

*Research was supported by Institut Teknologi Bandung Research Grant 2022, S. Bandong is supported by the Indonesia Endowment Fund for Education (LPDP), Indonesia.

S. Bandong is with the Engineering Physics Doctoral Program, Faculty of Industrial Technology, Institut Teknologi Bandung, Indonesia (e-mail: bandong.steven@gmail.com).

Y. Yunazwin Nazaruddin is with the Instrumentation and Control Research Group, Faculty of Industrial Technology, Institut Teknologi Bandung, Indonesia and National Center for Sustainable Transportation Technology, Institut Teknologi Bandung, Indonesia (e-mail: yul@tf.itb.ac.id).

E. Joelianto is with the Instrumentation and Control Research Group, Faculty of Industrial Technology, Institut Teknologi Bandung, Indonesia and National Center for Sustainable Transportation Technology, Institut Teknologi Bandung, Indonesia (e-mail: ejoel@tf.itb.ac.id).

container. m_1 has kinetic energy (T_1) and Potential Energy (P_1) as follows:

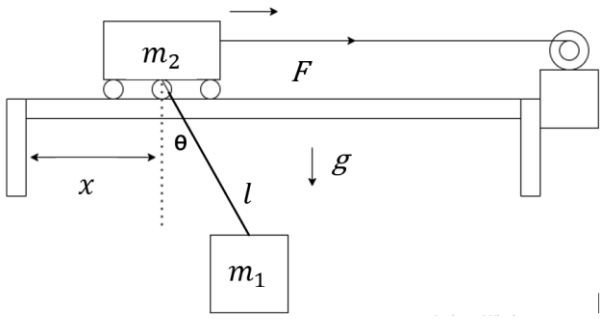

Figure 1. 2D Gantry Crane representation

$$T_1 = \frac{1}{2} m_1 \left(\dot{x}^2 + l^2 \dot{\theta}^2 + 2\dot{x} l \dot{\theta} \cos\theta \right) \quad (1)$$

$$P_1 = -m_1 g l \cos\theta \quad (2)$$

assuming the position of the trolley as a reference, m_2 has zero potential energy (P_2=0) and its kinetic energy is:

$$T_2 = \frac{1}{2} m_2 \dot{x}^2 \quad (3)$$

Equations (1), (2) and (3) are substituted into (4) to obtain L which will be substituted in the Lagrange equation (5).

$$L = T - P \quad (4)$$

$$L = \frac{1}{2} m_1 \left(\dot{x}^2 + l^2 \dot{\theta}^2 + 2\dot{x} l \dot{\theta} \cos\theta \right) + \frac{1}{2} m_2 \dot{x}^2 + m_1 g l \cos\theta \quad (5)$$

$$\frac{d}{dt}\left(\frac{\partial L}{\partial q_i} \right) - \frac{\partial L}{\partial q_i} = Q_i \quad (6)$$

Substitution of L in (6) will result in the dynamic equation of the 2D RTGC model.

$$(m_1 + m_2)\ddot{x} + m_1 l \ddot{\theta} \cos\theta - m_1 l \dot{\theta}^2 \sin\theta + D\dot{x} = F \quad (7)$$

$$m_1 l^2 \ddot{\theta} + m_1 l \ddot{x} \cos\theta + m_1 \dot{x} l \dot{\theta} \sin\theta + m_1 g l \sin\theta = 0 \quad (8)$$

RTGC dynamic models (7) and (8) are integrated with the motor model (9) to obtain a complete RTGC model. Details of getting the motor model can be seen in [8].

$$V = \left(\frac{R.r_p}{K_t.r} \right) F + \frac{K_e.r}{r_p} \dot{x} \quad (9)$$

Substituting (7) to (9) to obtain a nonlinear RTGC model driven by a DC motor:

$$V = \left(\frac{R.r_p}{K_t.r} \right)(m_1 + m_2)\ddot{x} + \left(\frac{D.R.r_p}{K_t.R} + \frac{K_e.r}{r_p} \right)\dot{x} + \left(\frac{m_1 l.R.r_p}{K_t.r} \right) \left(\ddot{\theta} \cos\theta - \dot{\theta}^2 \sin\theta \right) \quad (10)$$

$$l^2 \ddot{\theta} + l\ddot{x} \cos\theta + gl \sin\theta = 0 \quad (11)$$

For computational and simulation needs, (10) and (11) are linearized using the assumption of a small angle ($\theta \approx 0$), and $\sin\theta \approx \theta$, $\cos\theta \approx 1$, and $\dot{\theta}^2 \approx 0$. (12) and (13) are equations of the RTGC system and its driving motor after linearization.

$$V = \left(\frac{R.r_p}{K_t.r} \right)(m_1 + m_2)\ddot{x} + \left(\frac{D.R.r_p}{K_t.R} + \frac{K_e.r}{r_p} \right)\dot{x} + \left(\frac{m_1 l.R.r_p}{K_t.r} \right)\ddot{\theta} \quad (12)$$

$$l^2 \ddot{\theta} + l\ddot{x} + gl\theta = 0 \quad (13)$$

III. Robust PID H_∞ Integral Backstepping

The standard PID control equation is as follows:

$$u(t) = K_1 \int_0^t e(t)dt + K_2 e(t) + K_3 \frac{d}{dt} e(t) \quad (14)$$

where K_p, K_i, K_d are proportional, integral, and derivative constants. $e(t) = y(t) - r(t)$ is the difference between the set point $r(t)$ and process variable $y(t)$, u(t) is the PID controller signal. The state space system equation is:

$$\dot{x}(t) = Ax(t) + B_2 u(t)$$
$$y(t) = Cx(t) \quad (15)$$

where *x(t)* is the state. Equation (15) can be differentiated twice as stated in (16).

$$y = Cx$$
$$\dot{y} = CAx + CB_2 u$$
$$\ddot{y} = CA^2 x + CAB_1 u + CB_2 \dot{u} \quad (16)$$

Based on (16), the representation (14) becomes (17). Equation (18) gives the value K so that the control law is obtained as in (19).

$$\left(1 - K_3 CB_2\right)\dot{u} - \left(K_3 CA^2 + K_2 CA + K_1 C\right)x - \left(K_3 CAB_2 + K_2 CB_2\right)u = 0 \quad (17)$$

$$\hat{K}^T = \begin{bmatrix} \hat{K}_1 & \hat{K}_2 & \hat{K}_3 \end{bmatrix}^T = \left(1 - K_3 CB_2\right)^{-1} \begin{bmatrix} K_1 & K_2 & K_3 \end{bmatrix}^T \quad (18)$$

$$\dot{u} = \hat{K}^T \begin{bmatrix} C^T & A^T C^T & \left(A^2\right)^T \end{bmatrix}^T x + \hat{K}^T \begin{bmatrix} 0 & B_2^T C^T & B_2^T A^T C^T \end{bmatrix}^T u \quad (19)$$

Equation (18) applies if $\left(1 - K_3 CB_2\right)$ is not equal to zero. Equation (19) is written in a simpler form as follows:

$$u = K_a x_a(t) \quad (20)$$

where

$$u_a(t) = \dot{u}(t), \quad x_a(t) = \begin{bmatrix} x(t) \\ u(t) \end{bmatrix}$$

$$K_a = \begin{bmatrix} C^T & A^T C^T & \left(A^2\right)^T \\ 0 & B_2^T C^T & B_2^T A^T C^T \end{bmatrix} \hat{K} = \Gamma \hat{K} \quad (21)$$

$x_a(t)$ is the augmentation state associated with the following augmented system

$$\dot{x}_a(t) = A_a x_a(t) + B_a u_a(t) \quad (22)$$

where,

$$A_a = \begin{bmatrix} A & B_2 \\ 0 & 1 \end{bmatrix}; \quad B_a = \begin{bmatrix} 0 \\ 1 \end{bmatrix} \quad (23)$$

In case, (21) is not a rectangular matrix, the pseudo inverse method is used to find the inverse value or optimization can be applied to find the optimal pseudo inverse parameter. This paper uses H_∞ to form a robust PID controller. The state-space equation (15) under the influence of disturbance or uncertainty ($w(t)$) is represented in (24), where $z(t)$ is the objective state.

$$\sum = \begin{Bmatrix} \dot{x}(t) = Ax(t) + B_1 w(t) + B_2 \xi(t) \\ z(t) = \begin{bmatrix} C_1 x(t) \\ D_{12} \xi(t) \end{bmatrix} \end{Bmatrix} \quad (24)$$

An augmented model with an integrator ($\xi(t)$) added to the control signal is known as a backstepping integrator.

$$\sum = \begin{Bmatrix} \begin{bmatrix} \dot{x}(t) \\ \dot{\xi}(t) \end{bmatrix} = \begin{bmatrix} A & B_2 \\ 0 & \rho_2 I \end{bmatrix} \begin{bmatrix} x(t) \\ \xi(t) \end{bmatrix} + \begin{bmatrix} B_1 \\ 0 \end{bmatrix} w(t) + \begin{bmatrix} 0 \\ 1 \end{bmatrix} u_a(t) \\ z(t) = \begin{bmatrix} C_1 & 0 \\ 0 & D_{12} \\ 0 & 0 \end{bmatrix} \begin{bmatrix} x(t) \\ \xi(t) \end{bmatrix} + \begin{bmatrix} 0 \\ 0 \\ \rho_1 \end{bmatrix} u_a \quad ,\rho_2 < 0 \end{Bmatrix} \quad (25)$$

Based on the augmented model (25), the Algebraic Riccati Equation solution has the following form

$$0 = X \begin{bmatrix} A & B_2 \\ 0 & \rho_2 I \end{bmatrix} + \begin{bmatrix} A' & 0 \\ B_2' & \rho I \end{bmatrix} X - X \left(\rho^{-2} \begin{bmatrix} 0 & 0 \\ 0 & I \end{bmatrix} - \gamma^{-2} \begin{bmatrix} B_1 B_1' & 0 \\ 0 & 0 \end{bmatrix} \right) X + \begin{bmatrix} C_1 C_1' & 0 \\ 0 & D_{12}' D_{12} \end{bmatrix} \quad (26)$$

Therefore, if $\gamma > 0$ and $\rho > 0$ obtained $X = X^T > 0$ and controller (K_a) is defined as in (27).

$$K_a = -\rho^{-2} B_a{}^T X \quad (27)$$

Equations (18), (21) and (27) are used for the synthesis of a robust PID controller using H_∞ integral backstepping. The detailed derivation of this method can be found in [13][15][16].

IV. Methods and Experiments

The nominal RTGC model is based on (12) and (13) using a prototype container mass of 1 Kg and a rope length of 0.5m. This paper attempts to design a sway angle and position control system using a robust PID on the RTGC amidst variations in mass and length of the hauling rope. The controller is expected to be able to follow the reference trajectory designed based on 3rd order ITAE [9]. ω is selected according to the value of the desired settling time in controlling the position of the trolley. On Fig. 3, the green line shows the designed reference trajectory according to (28).

$$X_{ref} = \frac{\omega^3}{s^3 + 1.75\omega s^2 + 2.15\omega^2 s + 1.5\omega^3} \quad (28)$$

PSO (100 particles, 1000 iterations), SA (20000 iterations) and GA (1000 generations) are used as the optimization method for the H_∞ integral backstepping parameter (Table 1). There are six parameter needs to be optimized, matrix B_1 (4 elements), ρ and γ (26). The ITSE cost function is used as an optimization objective as stated in (29). t_0 (0s) is the initial simulation time, t_1 (2.6s) is the rise time and t_2 (4.24s) is the settling time of the reference trajectory.

$$J = \int_{t_0}^{t_1} t\left(x - x_{ref}\right)^2 dt + \int_{t_1}^{t_{end}} t\left(\theta\right)^2 dt + \int_{t_2}^{t_{end}} t\left(x - x_{ref}\right)^2 dt \quad (29)$$

Fig 2 shows the proposed control system that this paper intends to achieve and solve. The robustness of the optimized controller will be tested with variations in mass (0.4 Kg, 1 Kg, and 1.6 Kg) and variations in rope length (0.25 m and 0.75 m). PSO-based PID controller optimization without robustness considerations is also shown as a comparison.

TABLE I. H_∞ INTEGRAL BACKSTEPPING OPTIMIZATION RESULTS

Params	Optimization Range	Optimization Results		
		PSO	SA	GA
B_1 [1]	0-1	0.98	0.44	0.99
B_1 [2]	0-1	0.99	0.93	0.59
B_1 [3]	0-1	1.00	0.05	0.99
B_1 [4]	0-1	0.04	0.45	0.47
ρ	0-10	0.29	0.11	1.19
γ	0-10	1.71	0.66	3.51

TABEL II. ROBUST PID SYNTHESIS RESULT

Objective	Controller	PRP	SARP	GARP	PP
Position	Kp	32.70	31.98	33.14	100
	Ki	28.52	32.16	11.87	0
	Kd	5.09	5.00	5.85	28.17
Sway	Kp	1.55	1.62	0.49	-1.82
	Ki	-0.57	-0.56	-0.65	-100
	Kd	1.03	1.09	1.15	-12.26
Cost Function J (29)		0.049	0.051	0.073	0.003

V. Results and Analysis

Table I shows the results of the optimization of the H_∞ integral backstepping parameter. Matrix B_1 has 4 elements where in Table I the square brackets signify the n-th element of matrix B_1 ($B_1[n]$). Referring to [17], the value of γ is required to be small in order to handle large uncertainties. This optimal parameter is used to find the robust parameter whose name is abbreviated, for simplification, according to the name of the optimization algorithm, PSO robust PID (PRP), SA robust PID (SARP), GA robust PID (GARP) as shown in Table II. As a comparison, PID has also been optimized using PSO, PSO-PID (PP), without the robust method, and the results are obtained in the column at the right end of Table II. On each control objective, position, and sway control, optimal PID parameter is presented. Cost function J as stated in (29) is used to evaluate the control performance of each optimization method.

Fig. 3 shows the results of position and sway control and its control signal using the optimization results of each method. PP seems to be able to follow the trajectory of the position better and minimize the swing angle more quickly, as confirmed by the lower cost function value (Table II). However, the PRP, SARP and GARP methods also give good results as shown in Fig. 3 and Table III. The peak amplitude of the sway controller in the robust method is generally smaller. In addition, PRP and SARP have position controllers with faster rise and settling times and acceptable overshoots.

Compared to PP, the robust method also provides a competitive average steady-state error for position and sway angle controller. The average steady-state error here is the average error after the settling time for each controller is reached up to the 10s. The difference in settling time is also very small, namely 0.76s, because the settling time for the PP position is 4.20 s, and the settling time for the SARP and PRP swing angles is 5.06s. Therefore, PP does have better control accuracy, but the robust PID method is quite competitive, especially PRP and SARP

The controller robustness test was applied by varying the mass of the container and the length of the rope, as shown in Fig. 4. PP becomes unstable when the mass and length of the rope vary (see the first column). PRP, SARP and GARP can provide robust control over rope length and mass variations. Columns 2 through 4 in Fig. 3 show that the three robust PID parameters can achieve set point positions and reduce swing angles even under the influence of mass and rope length uncertainties. Therefore, it can be concluded that the PID H_∞ integral backstepping method has succeeded in providing robust position and sway angle control performance.

Details of the performance of the robust PID controller are presented in Table IV. Settling time is a measure of the controller's ability because settling time is the time required to reach steady state. It also contains a minimum error of 0.02 m position error and 0.02 rad swing angle error. PRP provides better robustness because its settling time sway is faster than others. SARP had the second-best performance by a very small margin against PRP, 0.04 s. GARP tends to respond much slower, although it can still provide rogue performance. The best method is assessed based on the settling time on the sway because, generally, the sway is slower to reach steady state than its position response.

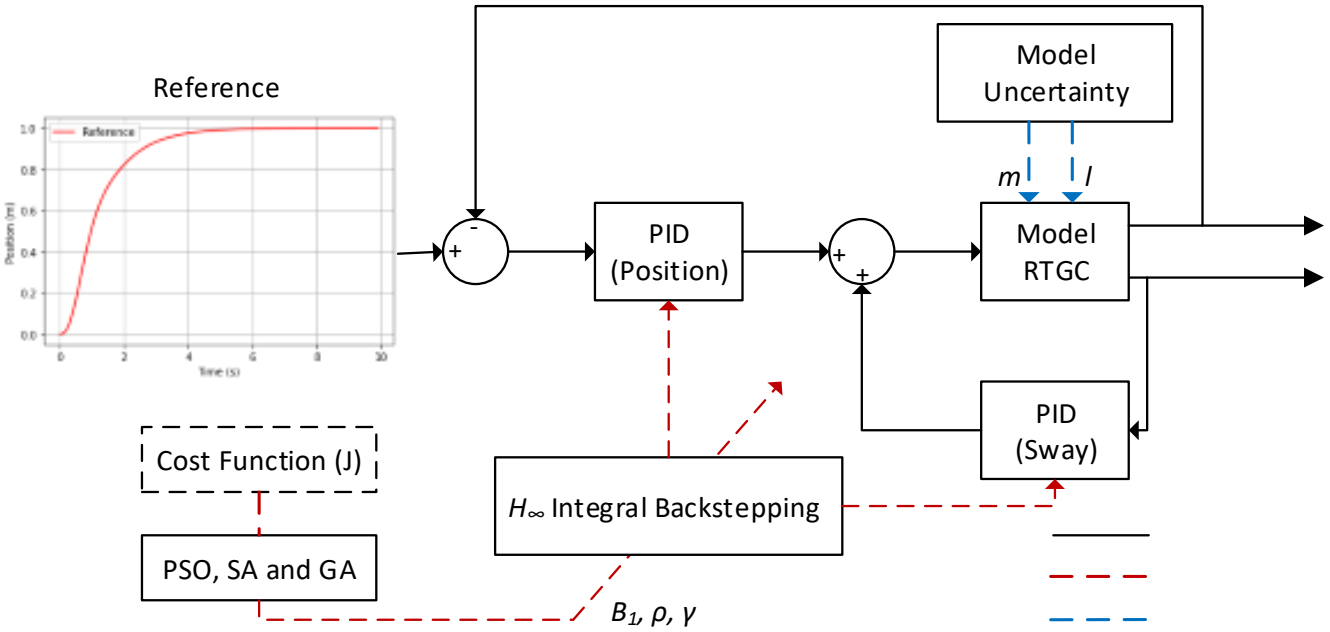

Figure 2. The Proposed Control System Design

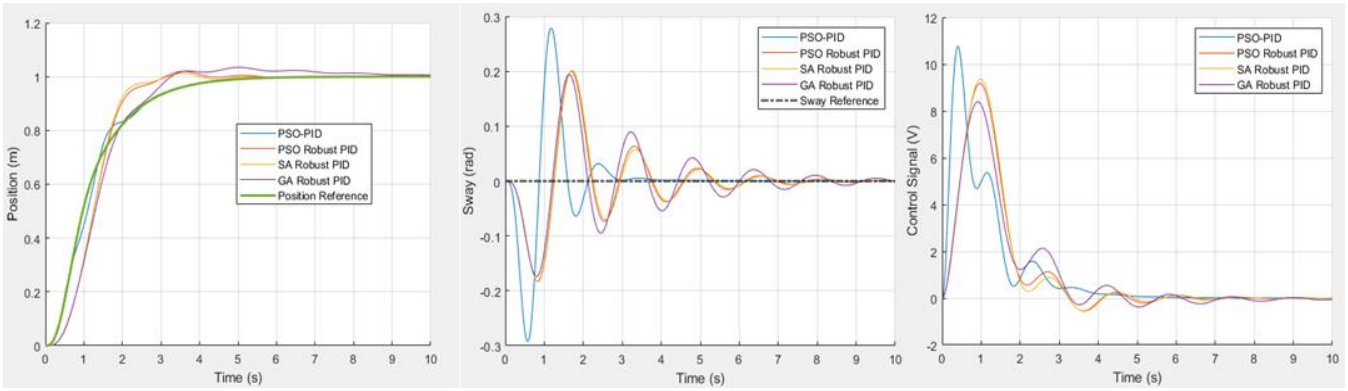

a. Position Control Response b. Sway Control Response c. Control Signal

Figure 3. Control Output with m =1 Kg and l =0.5 m

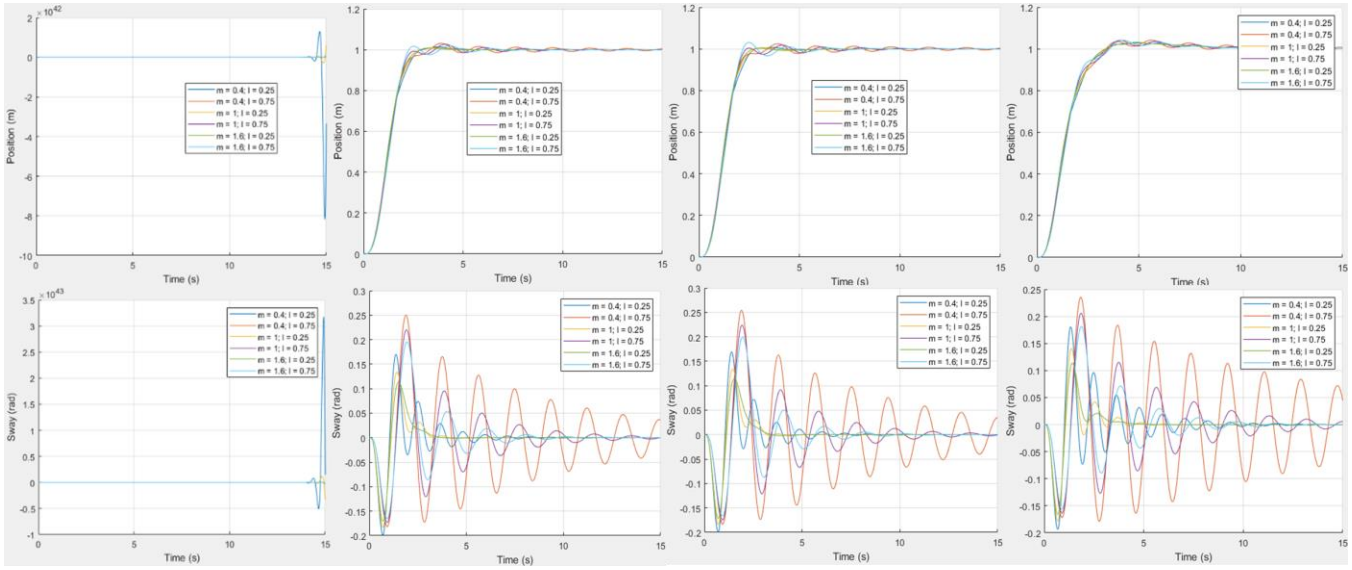

Figure 4. Robustness Test (1st Column: PP, 2nd Column: PRP, 3rd Column: SARP, 4th Column: GARP)

TABLE III. CONTROL PERFORMANCE METRICS

Method	Position				Sway			
	Rise Time (s)	Settling Time (s)	Overshoot (m)	Average SSE (m)	Settling Time (s)	Max Amplitude (rad)	Min Amplitude (rad)	Average SSE (rad)
PRP	2.84	2.84	1.02	0.003	5.06	0.20	-0.18	0.004
SARP	2.76	2.76	1.01	0.003	5.06	0.20	-0.18	0.004
GARP	3.09	6.83	1.03	0.010	6.45	0.19	0.17	0.006
PP	4.20	4.20	0	0.004	2.6	0.28	-0.29	0.001

TABLE IV. SETTLING TIME ROBUST PID UNDER UNCERTAINTY

Uncertainty		Position			Sway		
m (Kg)	l (m)	PRP (s)	SARP (s)	GARP (s)	PRP (s)	SARP (s)	GARP (s)
0.4	0.25	2.60	2.55	6.48	3.81	3.82	5.44
0.4	0.75	4.22	5.03	7.78	18.78	18.86	29.57
1.0	0.25	2.59	2.52	6.57	2.83	2.82	2.82
1.0	0.75	4.35	3.41	6.43	7.96	7.98	10.45
1.6	0.25	2.51	2.38	6.49	2.39	2.48	2.75
1.6	0.75	3.52	3.73	6.60	5.33	5.36	6.05
Average		3.30	3.27	6.72	6.85	6.89	9.51

VI. CONCLUSION

This paper considered a robust PID parameter based on the H_∞ integral backstepping method to control the position and sway angle of the RTGC. The H_∞ integral backstepping parameter was optimized using PSO, SA and GA to obtain a controller that can follow the desired trajectory. The obtained results indicated the ability of the robust PID controller to respond to mass and rope length uncertainties. The PID controller resulted from PSO and SA with H_∞ integral backstepping optimization provided better robustness than GA. Further research will consider other disturbances and uncertainties and apply them to the control of the RTGC prototype.

REFERENCES

[1] R. J. Sánchez, J. Hoffmann, A. Micco, G. v Pizzolitto, M. Sgut, and G. Wilmsmeier, "Port efficiency and international trade: port efficiency as a determinant of maritime transport costs," Maritime economics & logistics, vol. 5, no. 2, pp. 199–218, 2003.

[2] K. H. Kim and H.-O. Günther, "Container terminals and terminal operations," in Container Terminals and Cargo Systems, Springer, 2007, pp. 3–12.

[3] P. G. Ardi, A. G. Ayu, and others, "Safety management on loading process with rubber tyred gantry crane: case study at port of Tanjung Priok," Russian Journal of Agricultural and Socio-Economic Sciences, vol. 66, no. 6, pp. 150–164, 2017.

[4] N. B. Almutairi and M. Zribi, "Fuzzy controllers for a gantry crane system with experimental verifications," Mathematical Problems in Engineering, vol. 2016, 2016.

[5] M. I. Solihin, Wahyudi, and A. Legowo, "Fuzzy-tuned PID anti-swing control of automatic gantry crane," Journal of Vibration and Control, vol. 16, no. 1, pp. 127–145, 2010.

[6] J. Jafari, M. Ghazal, and M. Nazemizadeh, "A LQR optimal method to control the position of an overhead crane," IAES International Journal of Robotics and Automation, vol. 3, no. 4, p. 252, 2014.

[7] Ü. Önen and A. Çakan, "Anti-swing control of an overhead crane by using genetic algorithm based LQR," International Journal of Engineering And Computer Science, vol. 6, no. 6, 2017.

[8] S. Bandong, M. R. Miransyahputra, Y. Setiaji, Y. Y. Nazaruddin, P. I. Siregar, and E. Joelianto, "Optimization of Gantry Crane PID Controller Based on PSO, SFS, and FPA," in 2021 60th Annual Conference of the Society of Instrument and Control Engineers of Japan (SICE), 2021, pp. 338–343.

[9] M. I. Solihin, A. Legowo, R. Akmeliawati, and others, "Robust PID anti-swing control of automatic gantry crane based on Kharitonov's stability," in 2009 4th IEEE Conference on Industrial Electronics and Applications, 2009, pp. 275–280.

[10] Y. Y. Nazaruddin, A. D. Andrini, and B. Anditio, "PSO based PID controller for quadrotor with virtual sensor," IFAC-PapersOnLine, vol. 51, no. 4, pp. 358–363, 2018.

[11] Y. Y. Nazaruddin, A. N. Aziz, and O. Priatna, "Improving performance of PID controller using artificial neural network for disturbance rejection of high pressure steam temperature control in industrial boiler," in 2008 International Conference on Control, Automation and Systems, 2008, pp. 1204–1207.

[12] A. Gambier and Y. Y. Nazaruddin, "Collective pitch control with active tower damping of a wind turbine by using a nonlinear PID approach," IFAC-PapersOnLine, vol. 51, no. 4, pp. 238–243, 2018.

[13] E. Joelianto, L. E. Suryana, A. Widyotriatmo, and Y. A. Hidayat, "Optimal Control Strategy for Automated People Mover System using Robust H∞ Integral-Backstepping MIMO PID Controller".

[14] M. R. Katebi, M. J. Grimble, and Y. Zhang, "H∞ robust control design for dynamic ship positioning," IEE Proceedings-Control Theory and Applications, vol. 144, no. 2, pp. 110–120, 1997.

[15] A. Putri and E. Joelianto, "Robust H∞ Integral-Backstepping PID Controller for Hydropower System," in 2021 International Conference on Instrumentation, Control, and Automation (ICA), 2021, pp. 49–54.

[16] E. Joelianto and A. Bartosazewicz, "Robust H∞ PID Controller Design Via LMI Solution of Dissipative Integral Backstepping with State Feedback Synthesis," in Robust Control, Theory, and Applications, InTech Open Publ, 2011.

[17] K. Glover, "H-Infinity Control," Encyclopedia of Systems and Control, pp. 1–9. 2013.